

# Preparation and characterization of two modified laterite soils for arsenic removal in aqueous solutions: Efficiency and kinetic Modelling

## ABSTRACT

Consumption of arsenic-contaminated water is the cause of major problems such as melanosis, hyperkeratosis and cancer. To mitigate this pollution, this study was carried out using analytical methods to prepare chemically treated laterite (TL) and laterite chemically doped with ferrihydrite (DL). The adsorbents were characterised using scanning electron microscopy (SEM), X-ray diffraction (XRD), Fourier transform infrared spectroscopy (FTIR), inductively coupled plasma atomic emission spectrometry (ICP-AES), X-ray fluorescence (XRF) and the Brunauer Emmett Teller (BET) method. The specific surface area, bulk density and pH at zero charge point (pHpzc) of TL and DL ranged from 81.306 to 40.099 m<sup>2</sup>/g, from 1.67 to 2.27 and from 5.41 to 8.02, respectively. The SiO<sub>2</sub>/(Fe<sub>2</sub>O<sub>3</sub> + Al<sub>2</sub>O<sub>3</sub>) ratio was 0.31 for TL and 0.20 for LD, showing that the materials prepared were still classified as laterite adsorbents. The experimental results of batch experiments on the removal of arsenic (As (III)) and arsenic (As (V)) using the two adsorbents showed the strong influence of operating conditions such as pH, initial concentration, adsorbent dose and contact time. The Langmuir isotherm described the arsenic removal process indicating that monolayer adsorption occurred at located sites. For the removal of As(V), the maximum adsorption capacity was 7.36 and 9.79 mg/g for TL and DL, respectively, while for the removal of As (III), the adsorption capacity for TL and DL was 5.17 and 7.89 mg/g, respectively. The kinetic study of the adsorption of As(V) or As(III) on modified laterites concluded that the process was described by the pseudo-second-order model, with a chemisorption process to be explored.

**Keywords:** Adsorbent, Arsenic, Adsorption, Ferrihydrite, Laterite, Removal

## 1.INTRODUCTION

The alteration of rocks, whether due to natural processes or human activities, can result in the release of heavy metals and metalloids like arsenic into the environment [1,2]. Drinking water contaminated with arsenic can have effects on health such as pigmentation, hyperkeratosis, and ulceration), as well as respiratory, pulmonary, cardiovascular, gastrointestinal, hematological, hepatic, renal, reproductive, and immunological changes [3,4]. Arsenic exists in two common forms: As (III) and As (V), with As (III) being less commonly found in water but more toxic than As (V) [2,4]. Research conducted by Bretzler *et al.* [5] revealed that approximately 560,000 individuals in Burkina Faso may be at risk of exposure to

arsenic-contaminated water. Previous works showed some cases of hyperkeratosis and melanosis have been observed in several villages of Burkina Faso, including Tanlili, Essakane, and Mogtédó [6,7]. To address this public health concern, various techniques have been developed to reduce the level of arsenic in water including filtration, coagulation precipitation, reverse osmosis, electro dialysis, adsorption, and combination methods [4,8]. Adsorption, in particular, is shown as an effective method for treating water contaminated with arsenic, especially using adsorbent materials [8,9]. Among the adsorbent's materials, ferrihydrite is one of the more efficient, and widely used due to its specific physicochemical properties in removing both As (III) and As (V) [10,11]. However, the cost of preparation, limited availability of chemicals, and regeneration of ferrihydrite restrict its use in developing countries. Previous studies have explored the use of Balkuy laterite in treating arsenic-contaminated water [12,13]. Previous studies demonstrated that raw laterite collected in Balkuy district, showed a certain potential as an adsorbent of arsenic [14]. Moreover, prior research has demonstrated a significant correlation between the adsorption affinity of adsorbents rich in iron and arsenic [10,15]. The literature suggests that chemical pretreatment methods are effective in fixing ferrihydrite onto adsorbents [15,16,17]. Therefore, this study aimed to evaluate the efficiency of Balkuy laterite doped with ferrihydrite for arsenic removal from water.

The objective of this study was to contribute to the provision of safe drinking water in Burkina Faso by using locally available materials to treat arsenic-contaminated water. By studying the arsenic removal under various conditions, the mechanisms and kinetics of arsenic removal in batch mode were investigated under various operating parameters.

## **2. MATERIALS AND METHODS**

### **2.1. Chemicals**

1000 ppm stock solution of arsenic (III) was prepared following to the method of Pierce *et al.* [10] by dissolving sodium arsenite salt ( $\text{NaAsO}_2$ ) with a 20% NaOH solution (Flucka). The solutions of arsenic (III) and arsenic (V) were prepared from the stock solutions of  $\text{NaAsO}_2$  (Flucka) and  $\text{Na}_2\text{HAsO}_4 \cdot 7\text{H}_2\text{O}$  (Merck), respectively, in ultra-pure distilled water for the different adsorption tests. These solutions were stored at 4°C in until used. NaOH (Flucka) and  $\text{HNO}_3$  (Sigma-Aldrich) reagents prepared in analytical grade (AR) were used to adjust the pH of the matrix solutions. The pH of arsenic solutions was adjusted between 7 and 8 using 1M NaOH and/or 1M  $\text{HNO}_3$  with a pH- meter (HANNA, waterproof HI98318).

### **2.2. Preparations of Adsorbents**

The raw laterite was collected in Balkuy district (12°17'23.35" N, 1°27'46.90" W), located close to Ouagadougou (Burkina Faso). The chemically treated laterite (TL) and the ferrihydrite-doped treated laterite (DL) were prepared according to the method described by of Dehouet *et al.* [16]. The grain size below 75  $\mu\text{m}$  of the prepared adsorbents was used in the different tests. Mineral phases of raw laterite have been previously determined [14].

### 2.3. Physico-chemical characterization of adsorbents

Chemical analyses of the modified laterites were carried out by ICP-OES at the Bureau of Mines and Geology of Burkina (BUMIGEB). Experimentally, to 10g of laterite, were added 5mL of nitric acid (68%, Flucka), 10mL of hydrochloric acid (37%, Honeywell) and 5mL of fluoridric acid. The mixture was placed on a hot plate at  $175 \pm 5$  °C until a cake formed in the 100mL flask. The cake was then digested with 10 mL HCl and diluted with distilled water to the mark. The resulting solution was then diluted with distilled water. The structural morphology and surface chemical composition of the TL and DL adsorbents were analyzed using a scanning electron microscopy coupled with energy dispersive spectroscopy (SEM-EDS, Microspec-WDX 600/OXFORD). The Brunauer, Emmett, and Teller (BET) method was used to determine the specific surface area, Langmuir surface area, porosity, and pore size of TL and DL using a Micromeritics surface and pore size analyzer (TriStar II plus version 3.02). The surface functional groups of TL and DL were assessed by Fouriertransform -infrared spectroscopy (FTIR, OUAFO driven by OPUS software) in the range of 4000 to 400  $\text{cm}^{-1}$ . The powder of the modified laterites were determined by X-ray diffraction (XRD) using a Shimadzu XRD 6000 instrument. The scanning rate was set at  $2 \text{ min}^{-1}$  with a  $2\theta$  range between  $0^\circ$  and  $90^\circ$  [17,18]. To assess the amount of metal oxides present, Energy-Dispersive X-ray Fluorescence (EDXRF) was used to analyze the TL and DL adsorbents. Samples were irradiated by X-rays generated from the  $^{109} \text{Cd}$  annular source. The Si (Li) detector (Canberra), cooled with liquid nitrogen, allowed for the detection of the characteristic X-ray radiation of the sample. The spectrum was collected using the Genie-2000 software (Canberra, Meriden, CT, USA). The WinAxil version 4.5.2 software (Canberra Eurisys Benelux, Belgium) was used to analyze the spectral data. Quantitative evaluation was performed using the characteristic  $L\alpha$  lines of the elements. The bulk densities ( $d$ ) of the modified laterites were measured using a method described elsewhere [17]. The calculation of bulk density was performed using the following formula:

$$d = \frac{(m_1 - m_0)}{V} \quad (1)$$

The pH at the point of zero charge ( $\text{pH}_{\text{PZC}}$ ) value was determined from the curve (initial pH – final pH) as a function of the initial pH intercepting the x-axis of  $\text{pH}_i - \text{pH}_f = 0$  [19].

### 2.4. Arsenic Removal Experiments

Batch experiments were conducted to assess the adsorption capacity and performance of the prepared adsorbents in removing As (III) and As (V). Experiments were carried out using a rotary mechanical shaker at 150 rpm at the laboratory's ambient temperature of  $24 \pm 0.15^\circ\text{C}$  for 24 hours. An adsorbent dose of 4g/L of TL or DL with a concentration of 5mg/L of As (III) or As (V) was agitated with initial pH values adjusted between 2 to 12. The performance of modified laterites was evaluated by varying the mass dose over a range of 4 g/L to 14g/L with a solution concentration of 5 mg/L of As (V) or As (III). The chemical equilibrium was studied by varying the initial concentration of As (V) or As (III) from 1mg/L to 16 mg/L with an adsorbent dose of 4g/L of LT and LD. Adsorption kinetics experiments of As (III) or As (V) on TL and DL were conducted by performing tests from 01 to 24 hours with an

adsorbent dose of 4g/L and As concentration of 5 mg/L. The residual arsenic was analyzed using a Microwave Plasma-Atomic Emission Spectrometer (MP-AES Agilent 4200) after filtration [20]. The adsorption efficiency of the prepared adsorbents on As (V) or As (III) was evaluated through the removal rate denoted As (%) and the adsorption capacity denoted  $Q_e$  (mg/g).

The removal percentage (%As) was calculated using the following relationship:

$$As (\%) = \frac{C_i - C_e}{C_i} \times 100 \quad (2)$$

The adsorption capacity ( $Q_e$ ) was determined by the following formula:

$$Q_e \left( \frac{mg}{g} \right) = \frac{(C_i - C_e) \times V}{m} \quad (3)$$

### 3. RESULTS AND DISCUSSION

#### 3.1. Physico-Chemical Characteristics of prepared adsorbents

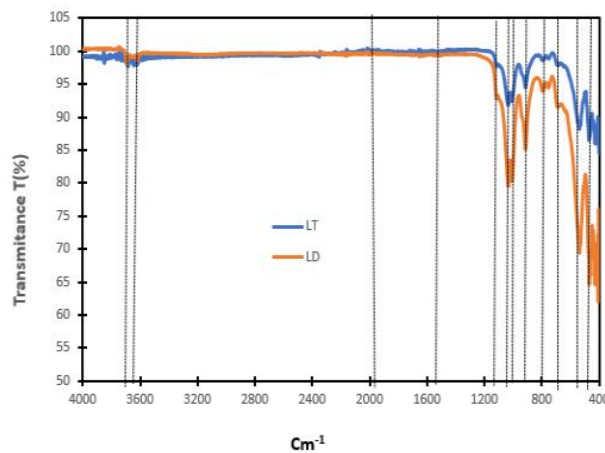
The physical parameters of prepared adsorbents were presented in Table 1. From the results, no significant change was observed in the total pore volume of the treated laterite vs the raw material. The increase in the value of density for LD was demonstrated through the contribution of iron during the doping of LT. Doping of LT by ferrihydrite has caused the closure of small pores by the binding of iron hydroxyls on the surface of these pores. In addition, the doping of TL by ferrihydrite has changed the surface charge, and the pH at the point of zero charge ( $pH_{PZC}$ ) from acidic 5.41 to alkaline pH of 8.02 [17]. Regarding surface characteristics, the total specific surface area of DL has been reduced by half after the treatment. We observed a decrease in the BET and Langmuir surface values after LT doping, indicating a preference for iron hydroxyls to bind to the BET and Langmuir surfaces rather than the external surface. These results are in agreement with the studies of Glocheux *et al.* [18], who showed that porous materials such as treated laterite have an external surface and negligible porosity compared to the internal structure, hence the fixation of iron hydroxyls on the internal surface (BET and Langmuir surface). The variations in the values of physical parameters indicated that the doping of laterite with ferrihydrite contributes to physicochemical changes [18, 21].

**Table 1: physical characteristics of TL and DL adsorbents**

Physical parameters	Quantitative values	
	LTLD	
Particle size ( $\mu m$ )	$\leq 75 \mu m$	
Density (d)	1.670 2.270	
pH at zero point of charge $pH_{pzc}$	5.410	8.020
Specific surface area BET ( $m^2/g$ )	24.548	7.995
Specific surface area of Langmuir ( $m^2/g$ )	30.208	10.688

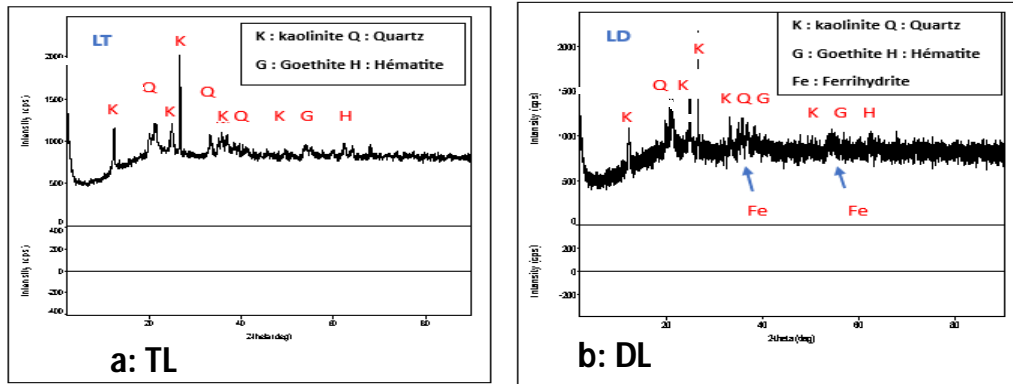
Specific external surface area (m <sup>2</sup> /g)	26.550	21.416
Total specific surface area (SS) (m <sup>2</sup> /g)	81.306	40.099
Total pore volume (cm <sup>3</sup> /g)	0.059	0.056

Figure 1 shows the surface functional groups of prepared adsorbents. Three zones of characteristic spectral bands are observed. The vibration zone around 3700-3300 cm<sup>-1</sup> corresponds to the -OH functional group. Three distinct peaks represent the bonds with Al<sup>3+</sup>, Fe<sup>2+</sup>, Fe<sup>3+</sup>, and Ti<sup>4+</sup> such as Fe-O, Al-O, Ti-O in the surface of the adsorbents [18,21]. The second spectral band zone, the broad band around 1634 cm<sup>-1</sup>, is attributable to isolated and bound water molecules on the adsorbents. The broad peak around 2005 cm<sup>-1</sup> on TL adsorbent is due to CO<sub>2</sub> adsorption [18]. The peaks around 1096, 910, 790, and 910 cm<sup>-1</sup> confirmed the presence of characteristic Si-O bonds for both TL and DL adsorbents [22]. However, the bands around 530 and 460 cm<sup>-1</sup> correspond to the vibration of the Fe-O bond of TL and DL [21,22]. The intensity of the transmittance bands of the TL adsorbent was attenuated compared to the DL after doping.



**Figure 1:** FT-IR surface function analysis of TL and DL adsorbents

XRD analysis of TL and DL adsorbents showed that there were structural modifications after doping the treated laterite (Figure 2a and 2b). Attributions of 2 $\theta$  diffraction peaks to mineral phases were made through Powder Diffraction File Data Maps (PCPDF no. 290173 and 290712), available in the literature[18,21]. Results revealed the presence of kaolinite, quartz, goethite, and hematite in TL adsorbents. In DL, in addition to previously cited phases, a significant amount of amorphous phase of 2-line ferrihydrite was observed on the diffractogram. The changes the intensities of mineral phases in the diffractograms could indicate the performance of DL laterite for the adsorption of As (III) and As (V) compared with TL laterite[17].



**Figure 2:** Diffractogram of the mineral phases of TL and DL laterites

SEM analysis of TL and DL adsorbents by at 10.0 μm scale is given in Figure 3. Both adsorbents consist of irregularly agglomerated particles in the form of platelets. The platelets stacked on the TL and DL adsorbents would be the kaolinite [18]. The kaolinite platelets were less formed on DL comparatively to TL laterite. The incursions of whitish spherical shapes present on DL are probably attributable to goethite, hematite and ferrihydrite [21]. TL adsorbent exhibited larger pores compared to DL, which can be attributed to the presence of iron hydroxides from doping on distinct pore structures. This explained the increase in the specific surface area of TL compared to DL (Table 1). The results of FT-IR, XRD data, chemical analysis by ICP-OES, and metal oxide by EDXRF of the adsorbents were used to identify and quantify the elemental composition in the form of oxide [23]. Results were recorded in Table 2, which indicate that aluminum oxides, iron oxides, silica, and titanium are the main phases present in both adsorbents. The content of iron oxides was relatively higher in DL than TL, as a result of the fixation of iron after doping. A relative low value of silica, aluminum, and titanium in DL is due to the opening of pores during the fixation of iron oxides during the deposition of ferrihydrite [16,17].  $\text{SiO}_2/(\text{Fe}_2\text{O}_3 + \text{Al}_2\text{O}_3)$  ratio was 0.31 for LT adsorbent and 0.20 for LD adsorbent, which indicate that LT and LD adsorbents can still be classified as lateritic adsorbents [14, 22].

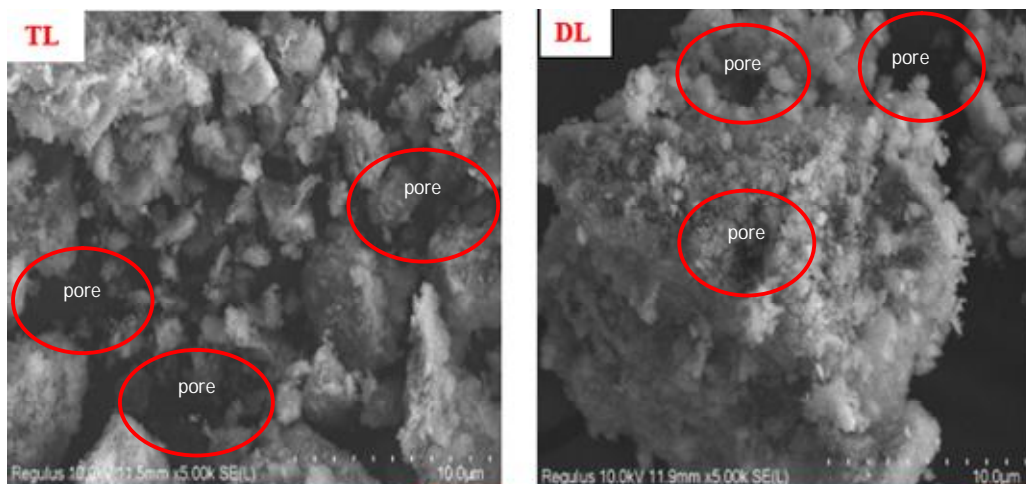
**Table 2:** Elemental chemical composition of TL and DL (% m/m)

Oxides	SiO <sub>2</sub>	Al <sub>2</sub> O <sub>3</sub>	Fe <sub>2</sub> O <sub>3</sub>	TiO <sub>2</sub>	N <sub>2</sub> O	MgO	CaO	ZnO, CuO, MnO <sub>2</sub>
TL	19.07	25.62	36.31	1.82	4.45	4.85	2.05	≤ 1
DL	13.67	18.31	51.04	0.17	4.24	4.34	208	≤ 1

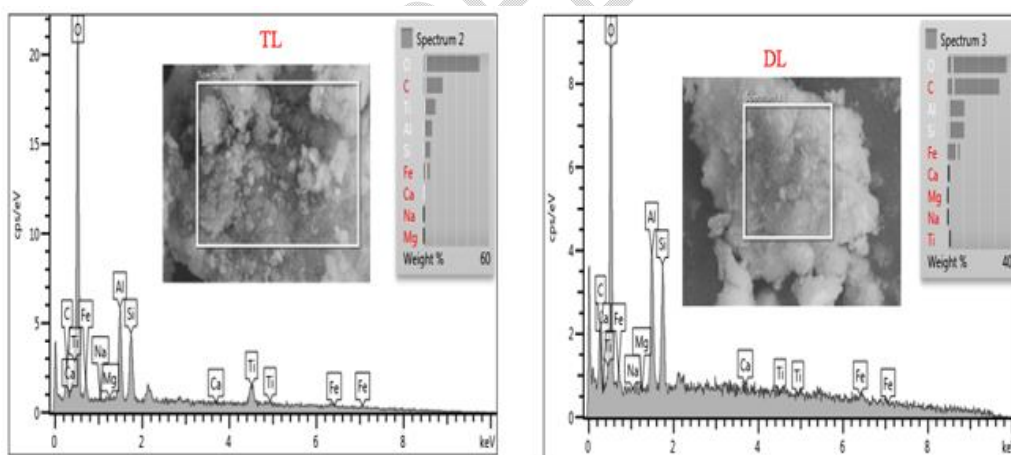
  

Elemental surface chemical analysis EDX								
O	C	Si	Al	Fe	Ti	Na	Ca	
LT	51.43	17.52	6.24	7.73	5.62	17.52	0.11	0.39
LD	37.29	32.71	10.60	10.74	7.69	*	0.05	0.86

\*Not determined



Elemental surface chemical analysis of the TL and DL adsorbents was conducted using a 2.5  $\mu\text{m}$  scale plate. Figure 4 displays the EDX spectra of TL and DL as qualitative analysis. The surface elemental chemical composition of LT and LD adsorbents as determined by EDS is presented in Table 2. The increase in silicon, carbon, iron, and aluminum content suggests that doping with ferrihydrite also improves the dispersion of these chemical elements in the adsorbent matrix. These EDS results provided further support for the XRD and EDXRF data. Moreover, the elemental composition of the prepared adsorbents was similar to other compositions reported in the literature [14,16,17].

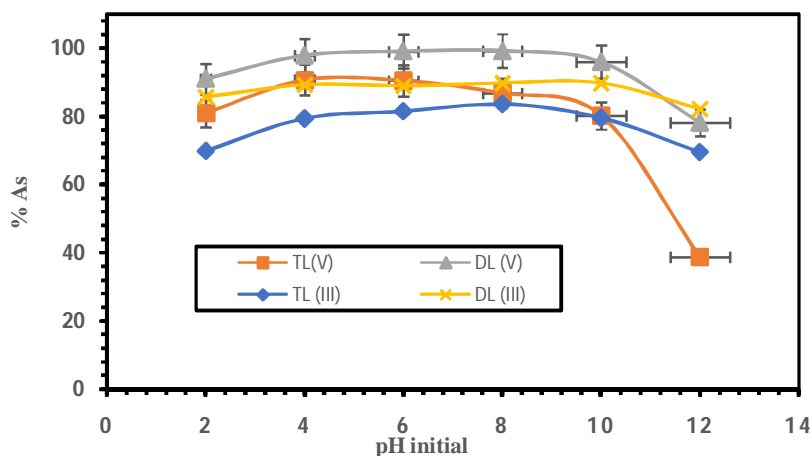


### 3.2. Effect of Operating Parameters on Arsenic Removal

#### 3.2.1. Effect of initial pH of solution

The effect of pH on the removal of As (III) and As (V) is presented in Figure 5. Optimal removal rate of As (V) on DL is achieved at a pH range between 4 and 8 with 99% of removal. Beyond a pH of  $\geq$

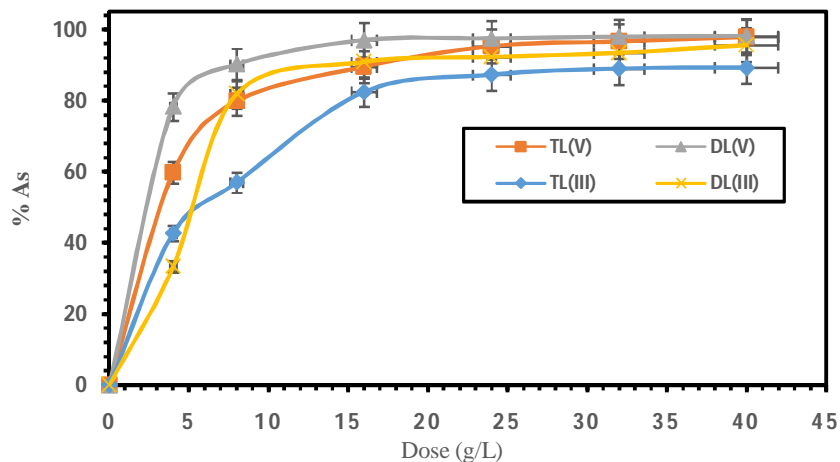
$\text{pH}_{\text{PZC}}$  (8.02) and at a pH below 4, the removal rate of As (V) gradually decreased. In contrast, using TL, the optimal pH was 5 with a removal rate of 90.30% of As (V). Above the  $\text{pH}_{\text{PZC}}$  (5.41) of TL, the removal rate of As (V) decreased from 88.98 to 38.86%. The removal of As (III) using adsorbents was not pH dependent in the range of pH = 2 to 10 because of its neutral form present in this pH range. The adsorption efficiency depends on the ionic forms of arsenic in solution ( $\text{H}_3\text{AsO}_4$ ,  $\text{H}_2\text{AsO}_4^-$ ,  $\text{HAsO}_4^{2-}$ ,  $\text{AsO}_4^{3-}$ ,  $\text{H}_3\text{AsO}_3$ ,  $\text{H}_2\text{AsO}_3^-$ ) and the adsorbents' point of zero charge ( $\text{pH}_{\text{PZC}}$ ). For  $\text{pH} \leq \text{pH}_{\text{PZC}}$  of adsorbents, the removal rate could be explained by the attraction process of the anionic forms of As (V) to the positively charged surface of adsorbents. On the other hand, beyond the  $\text{pH}_{\text{PZC}}$  of adsorbents, the decrease in the removal rate indicates some repulsion of ionic forms of As (V) and hydroxyl ions on the negatively charged surface of adsorbents [13,17]. Low removal rates for As (III) compared to As(V) at the same pH could be due to its stability at  $\text{pH} < 9.2$  and its neutral form ( $\text{H}_3\text{AsO}_3$ ) in solution, hence no electrostatic interaction on the surfaces [18]. The removal of As (III) on the surface of the adsorbents for pH comprised between 2 and 10 is mainly by ligand exchange, and



electrostatic interaction is insignificant [18, 21].

### 3.2.2. Effect of Adsorbent Dose

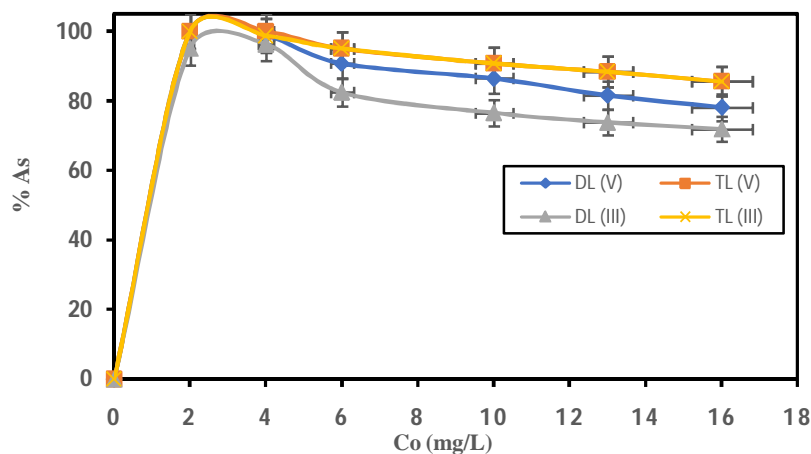
The effect of TL and DL dose on the removal of As (III) and As (V) was evaluated at adsorbent concentration from 4 to 40 g/L with an initial concentration of 5 mg/L at pH 7.05 for 24 hours contact time. Figure 6 showed the increase in the removal rate of As (V) and As (III) on both adsorbents. The removal rate of As (V) increased from 59.84 to 95.72% using TL and from 78.32 to 98.20% using DL with the increase in adsorbent dose. In contrast, the removal rate of As (III) increased from 42.76 to 89.30% and from 33.40 to 95.70% respectively for TL and DL. High performance of TL was reached at 24 g/L for 87.28% of As (III) and 95.34% of As (V). Using DL, the optimal removal was for 90.88% of As (III) and 97.08% of As (V) with 16 g/L. From this result, the increase of arsenic removal indicates a more favourable adsorption of As (III) and As (V) using both two laterites. The increase in the rate removal of arsenic forms using DL was attributed to the addition of active sites resulting from the doping of the TL adsorbent [10,15].



### 3.2.3. Effect of Initial Concentration

The adsorption behavior of As (V) and As (III) onto TL and DL was carried out by varying the concentration between 2 and 16 mg/L at pH 7.11 with an adsorbent dose of 4g/L during 24 hours contact time (Figure 7). The removal rate of As (V) decreased from 100 to 85.62% and from 100 to 78.12% respectively using TL and DL. By removing As (III), the removal rate evolved from 100 to 65.62% and from 95 to 56.87% using TL and DL, respectively. The optimal initial concentration of As (V) and As (III) was respectively 6 mg/L and 4mg/L using TL. Using DL, the optimal removal was obtained at a initial concentration of 2 mg/L for As (V) and As (III). High performance of TL compared to DL could be explained by its high total specific surface area (approximately twice that of DL,) to fix more arsenic ions in solution [21, 24]. The progressive decrease in the removal rate of As (V) and As

(III) is due to the limited number of active sites of the adsorbents during the increase in initial arsenic concentration [24].



### 3.2.3. Effect of Contact Time

The influence of contact time was evaluated over 24 hours with an initial pH of 7.09 using TL and DL. The Figure 8 shows the evolution of the removal rate of As (III) and As (V) according to two phases over time. During the first 4 hours, a rapid increase in the removal of As (III) and As (V) on the adsorbents was noted. For As (V), 79.47 and 95% of the removal rate were achieved using TL and DL, respectively. In contrast, the removal rate of As (III) was 39.45 and 79.47% using TL and DL, respectively. This rapid removal was due to the availability of free active sites of the adsorbents at the beginning of the adsorption process [14,17]. After 4 hours, the removal of As (III) and As (V) on the TL and DL laterites reached chemical equilibrium. The adsorption rate then remained constant. At equilibrium, the performance of DL was 97.67% and 100% for As (III) and As (V) respectively. Using TL laterite, the performance was 81.24% and 95.05% for As (III) and As (V) respectively at equilibrium time. This equilibrium performance of DL could be explained by the physicochemical surface properties allowing for the gradual removal of the initial concentration of As (III) and As (V) over time. The saturation of active sites of TL could be explained by the chemical equilibrium reached, indicating that it is not possible to increase the arsenic removal with the evolution of time [18, 24].

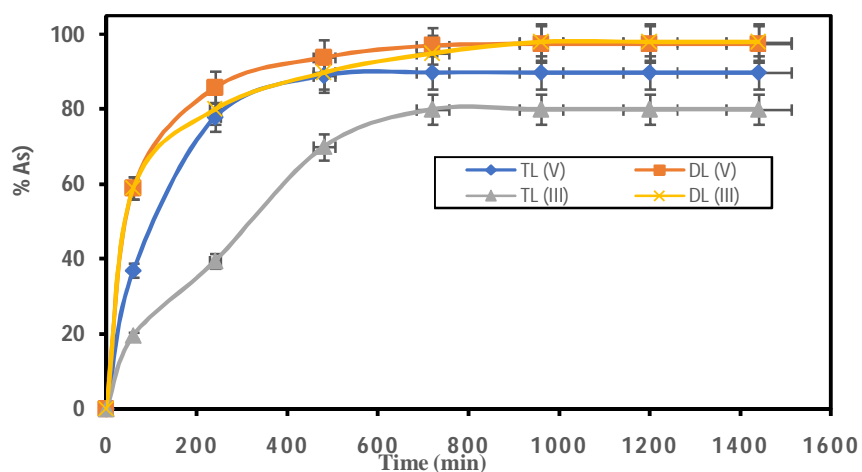


**Figure 8:** Effect of initial time on the removal of As (V) and As (III),  $C_0 = 5\text{mg/L}$ , dose =  $4\text{g/L}$ , and  $\text{pH} = 7.09$

### 3.2.4. Kinetic Modeling

To study the kinetic mechanism of treated laterite (TL) and doped laterite (DL), experimental data obtained with influence of contact time, were linearized with the models of pseudo-first order and pseudo-second order, respectively described by Lagergren *et al.* [25] and by Ho and McKay[26] for the adsorption of As (V) and As (III). The integration of the equations gives the following formulas respectively:

$$\ln(Q_e - Q_t) = -k_1 t + \ln Q_e \quad (4)$$

$$\frac{t}{Q_t} = \frac{1}{Q_e} t + \frac{1}{k_2 Q_e^2} \quad (5)$$

The representations of these equations are given by the Figure 9:

Values of the kinetic constants are listed in Table 3 where we noticed the experimental and theoretical capacity of each laterite. In addition, the values of correlation coefficient  $R^2$  is given for expected comparison.

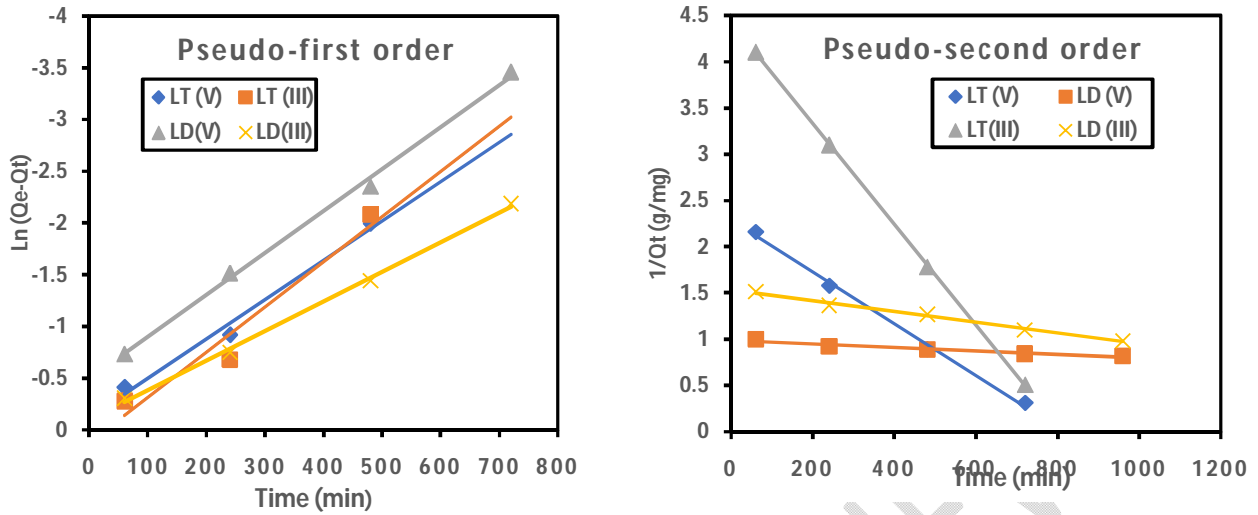


Table 3: Kinetic constants for pseudo-first and pseudo-second order

Pseudo-first order		Pseudo-second order						
Adsorbents		Adsorbents						
$Q_{e,exp}$	$Q_{e,theo}$	$R^2$	$Q_{e,exp}$	$Q_{e,theo}$	$R^2$			
mg/g	mg/g	$min^{-1}$	mg/g	mg/g	$min^{-1}$			
TL (V)	0.72	0.270	0.008	0.91	0.72	0.70	0.14	0.98
DL (V)	0.89	0.21	0.010	0.93	0.89	0.90	0.38	0.99
TL (III)	0.68	0.17	0.006	0.87	0.68	0.67	0.12	0.98
DL (III)	0.76	0.19	0.007	0.96				

Figure 9: Representation of the kinetic models of the removal of

The comparison between the experimental adsorption capacity ( $Q_{e,exp}$ ) and calculated ( $Q_{e,theo}$ ) of the first-order and pseudo-second-order is given in Table 3. Using the pseudo-second-order model, values of correlation coefficient ( $R^2$ ) were higher compared to the pseudo-first-order model. In addition, the calculated values of adsorption capacities  $Q_{e,theo}$  are close to the experimental values ( $Q_{e,exp}$ ) with the pseudo-second-order model. All these results indicated that the adsorption of As (III) and As (V) using two TL and DL adsorbents was described by the pseudo-second-order kinetic. The mechanism of As (III) and As (V) removal could then be describe by chemisorption process [17,27].

### 3.2.5. Adsorption Isotherms

The adsorption behavior of As (V) and As (III) onto TL and DL as a function of the initial concentration was linearized to the Langmuir and Freundlich isotherms [28,29]. The monolayer adsorption capacity on homogeneous active sites of TL and DL adsorbents was studied using the Langmuir model; and

multilayer adsorption on heterogeneous sites was evaluated using the Freundlich model for As (III) and As (V) [30]. The linearized form of the Langmuir isotherm model is given by the relation (6):

$$\frac{C_e}{Q_e} = \frac{1}{Q_m} (C_e) + \frac{1}{K_L Q_m} \quad (6)$$

The equation of the Freundlich model is given by the following relation (7):

$$\ln Q_e = \ln K_f + \frac{1}{n} \ln C_e \quad (7)$$

Figure 9 shows the plots  $C_e/Q_e = f(C_e)$  and  $\ln Q_e = f(\ln C_e)$  for Langmuir and Freundlich, respectively. The slopes and intercepts of the curves were used to calculate the various constants of isotherm models. Data of isotherm models are recorded in Table 4.

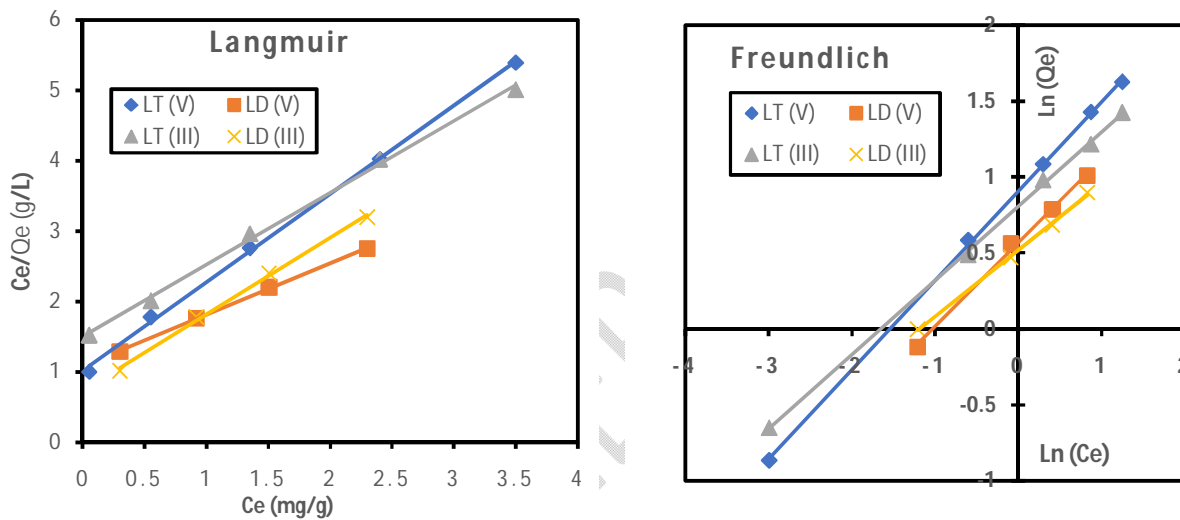


**Table 4:** Langmuir and Freundlich constants for the removal of As (III) and As(V) using TL and DL.

Adsorbent	Langmuir			Freundlich		
	$Q_m$ (mg/g)	$K_L$ (L/mg)	$R^2$	$K_f$ (mg/g)	$n$	$R^2$
TL(V)	7.36	0.73	0.98	5.06	1.78	0.97
DL (V)	9.79	0.28	0.99	6.31	3.46	0.98
TL (III)	5.17	1.01	0.99	2.98	1.09	0.98
DL (III)	7.89	0.38	0.99	4.01	2.72	0.99

**Figure 10:** Representation of the isotherm models of As (V).

The  $R^2$  constants of Langmuir and Freundlich isotherms are between 0.97 and 0.99 using TL and DL, indicating a good correlation and possible exploitation of experimental data for the removal of As (III) and As (V). The values of maximum capacities ( $Q_m$ ) and affinity constants ( $n$ ) of Langmuir and

Freundlich respectively recorded in Table 4 show an affinity and favorable reaction between the different mineral phases of the two adsorbents and the forms of arsenic. Consequently, the removal of As(III) and As(V) could be occurred by multilayer adsorption. The equilibrium parameter  $R_L$  and the Gibbs free energy ( $\Delta G$ ) were evaluated from the following relationships based on the Langmuir isotherm [29].

$$\Delta G = -RT \ln K_L \quad (8)$$

$$R_L = \frac{1}{1 + K_L C_0} \quad (9)$$

The calculated  $R_L$  values are between 0 and 1 with negative Gibbs free energies between 1.23 and 3.14 kJ/mole indicating the removal of As(III) and As(V) was occurred by adsorption following a reversible process onto TL and DL adsorbent [30,31].

#### 4. CONCLUSION

In this work, we reported the improvement of the properties of a laterite by analytical preparation techniques of TL and DL. Characterization by physico-chemical methods of the adsorbents allowed to observe structural modifications with surface functions. The presence of kaolinite, quartz, goethite, and hematite was observed on the treated laterite, and in addition to these mineral phases, ferrihydrite was identified on the doped treated laterite. Batch adsorption tests showed that the efficiency of TL and DL adsorbents in the removal of As (V) and As (III) depended on operating conditions (initial pH, adsorbent dose, initial concentration, and initial time). The mechanisms of removal of As (V) and As (III) on TL and DL were described by multilayer adsorption occurred onto heterogenous surfaces of DL and TL with not located sites. Kinetic study of adsorption of As (V) or As (III) onto adsorbents followed the pseudo-second-order model.

#### REFERENCES

- [1] Sayan, B.; Avishek, T.; Shubhalakshmi, S.; Tuyelee, D.; Abhijit, D.; Kaushik, G.; Nalok, D. Arsenic contaminated water remediation: A state-of-the-art review in synchrony with sustainable development goals. *Groundwater for Sustainable Development*. 2023, 23, 2352-801X. DOI: <https://doi.org/10.1016/j.gsd.2023.101000>.
- [2] Smedley, P. L.; Knudsen, J.; Maiga, D. Arsenic in groundwater from mineralized Proterozoic basement rocks of Burkina Faso. *Applied Geochemistry*. 2007, 22, 1074–1092. DOI: <https://doi.org/10.1016/j.apgeochem.2007.01.00>.
- [3] Ollé, R.K.; Corneille, B.; Inoussa, Z.; Boubié, G. Assessing the Source of Thallium Contamination in Ground and Surface Waters in the Locality of Yamtenga (Burkina-Faso): Correlation with Some Heavy

Metal Ions. *International Research Journal of Pure and Applied Chemistry*. 2019, 19, 1-14. <https://doi.org/10.9734/IRJPAC/2019/v19i430122>.

[4] Ackmez, M.; Sanjay, K.S.; Vinod, K.G.; Chin, H.T. Arsenic: An Overview of Applications, Health, and Environmental Concerns and Removal Processes. *Critical Reviews in Environmental Science and Technology*. 2011, 41, 435-519. DOI: <http://dx.doi.org/10.1080/10643380902945771>.

[5] Bretzler, A.; Lalanne, F.; Nikiema, J.; Podgorski, J.; Pfenninger, N.; Berg, M.; Schirmer, M. Groundwater arsenic contamination in Burkina Faso, West Africa: Predicting and verifying regions at risk. *Science of the Total Environment*. 2017, 614, 585-598. DOI: <https://doi.org/10.1016/j.scitotenv.2017.01.147>.

[6] Knudsen, J.; Pradelles, Y.; Zougouri, A. *Étude approfondie dans 8 villages de la région Nord ayant des forages à taux d'arsenic élevés*. Rapport du projet DANIDA / COWI, Ministère des affaires étrangères, Burkina Faso. 2005, 1-159.

[7] Somé, I.T.; Sakira, A.K.; Ouédraogo, M.; Ouédraogo, T. Z.; Traoré, A.; Sondo, B.; Guissou, I. P. Arsenic levels in tube-wells water, food, residents urine and the prevalence of skin lesions in Yatenga province, Burkina Faso. *Interdisciplinary Toxicology*. 2012, 5, 38-41. <https://doi.org/10.2478/v10102-012-0007-4>.

[8] Arunima, N.; Priya, C.; Brij, B.; Kapil, G.; Seema, S.; Mika, S. Removal of emergent pollutants: A review on recent updates and future perspectives on polysaccharide-based composites vis-à-vis traditional adsorbents. *International Journal of Biological Macromolecules*. 2024, 258, 0141-8130. DOI: <https://doi.org/10.1016/j.ijbiomac.2023.129092>.

[9] Sanou, Y.; Pare, S. Arsenic pollution through drinking groundwater in Burkina Faso: research of a cheap removal technology. In: M. Nolasco, E. Carissimi, E. Urquieta-Gonzalez (Eds.) *water perspectives in emerging countries: linking water security to sustainable development goals*. Cuvillier Verlag Göttingen, Inc., Germany. 2018, 137-148.

[10] Pierce, M.L.; Moore, C.B. Adsorption of arsenite and arsenate on amorphous iron hydroxide. *Water Resource*. 1982, 16, 1247-1253 DOI: [https://doi.org/10.1016/0043-1354\(82\)90143-9](https://doi.org/10.1016/0043-1354(82)90143-9).

[11] Yongfeng, J.; Liying, X.; Zhen, F.; George, P.; Demo, P. Observation of Surface Precipitation of Arsenate on Ferrihydrite. *Environmental Science Technology*. 2006, 40, 3248-3253. DOI: <https://doi.org/10.1021/es051872>.

[12] Sanou, Y.; Kabore, R.; Pare, S. Adsorption of arsenic and phosphate from groundwater onto a calcined laterite as fixed bed in column experiments. *French-Ukrainian Journal of Chemistry*. 2020 8(2), 227-242. <https://doi.org/10.17721/fujcV8I2P227-243>.

[13] Sanou, Y.; Tiendrebeogo, R.; Pare, S. Développement d'un pilote de traitement des eaux de forage contaminées par l'arsenic pour une application en zones rurales au Burkina Faso. *Journal of the West African Chemistry Society*. 2020, 49, 22-30.

- [14] Sanou, Y.; Kolawole, C.B.; Tiendrebeogo, R.; Kabore, R.; Tchakala, I.; Pare, S. Physico-chemical and spectroscopic properties of two laterite soils for applications in arsenic water treatment. *International Journal of Multidisciplinary Research and Development*. 2020, 7, 12-17.
- [15] Mahler, J.; Persson, I. Rapid adsorption of arsenic from aqueous solution by ferrihydrite-coated sand and granular ferric hydroxide. *Applied Geochemistry*. 2013, 37, 179-189. DOI: <https://doi.org/10.1016/j.apgeochem.2013.07.025>.
- [16] Dehou, S.C. *Etude des propriétés d'adsorption des oxyhydroxydes de fer déposé sur un support naturel (la brique) : application à l'élimination du fer dans les eaux de forages en République Centrafricaine*. Thèse, Université Lille 1. 2011, France.
- [17] Sanou, Y. *Etude de la performance des charbons actifs, du granulé d'hydroxyde ferrique et de la latérite pour l'élimination de la demande chimique en oxygène, du calcium et de l'arsenic des eaux*. Thèse de doctorat unique, Université Ouaga I Pr Joseph KI-ZERBO. 2017, Burkina Faso
- [18] Glocheux, Y.; Méndez, M.; Albadarin, B.; Allen, J.; Walker, M.G. Removal of Arsenic from Groundwater by Adsorption onto an Acidified Laterite By-Product. *Chemical Engineering Journal*. 2013, 228: 565–74. DOI: <https://doi.org/10.1016/j.cej.2013.05.043>.
- [19] Reymond, J.P.; Kolenda, F. Estimation of the point of zero charge of simple and mixed oxides by mass titration. *Powder Technology*. 1999, 103, 30–36. DOI: [https://doi.org/10.1016/S0032-5910\(99\)00011-X](https://doi.org/10.1016/S0032-5910(99)00011-X).
- [20] Azhar, A.G.; Zuhair, A. A. K.; Kasim, H. K. Selective extraction and determination of Arsenic (III) and Arsenic (V) in some food samples by cloud-point extraction coupled with hydride generation atomic absorption spectrometry. *International Research Journal of Pure et Applied Chemistry*. 2014, 4, 362-377.
- [21] Chatterjee, S.; De, S. Application of novel, low-cost, laterite-based adsorbent for removal of lead from water: Equilibrium, kinetic and thermodynamic studies. *Journal of Environmental Science and Health, Part A*. 2016, 51, 193-203. DOI: <https://doi.org/10.1080/10934529.2015.1094321>.
- [22] Boccuzzi, F.; Chiorino, A.; Manzoli, M.; Andreeva, D.; Tabakova, T. FTIR study of the low-temperature water–gas shift reaction on Au/Fe<sub>2</sub>O<sub>3</sub> and Au/TiO<sub>2</sub> catalysts. *Journal Catalysis*. 1999, 188, 176–185. DOI : <https://doi.org/10.1006/jcat.2001.3290>.
- [23] Njoya, D.; Njoya, A.; Kamlo, N.A.; Tchuidjang, Y.D.; Nkoumbou, C. Caractérisation chimique et minéralogique de quelques indices de bauxite de Fouban (Ouest-Cameroun). *International Journal of Biological and Chemical Sciences*. 2017, 11, 444. <https://doi.org/10.4314/ijbcs.v11i11.35>.
- [24] Tasrina, R.C.; Amin, M.N.; Quraishi, S.B.; Mustafa, A.I. Arsenic (III) Removal from Real-Life Groundwater by Adsorption on Neem Bark (*Azadirachta indica*). *International Research Journal of Pure et Applied Chemistry*. 2014, 46, 594-604

- [25] Abinashi,S.;Jeongwon,P.;Hyoeeun,K.; Pyung,K.P. Arsenic removal from aqueous solutions by adsorption onto hydrous iron oxide-impregnated alginate beads. *Journal of Industrial and Engineering Chemistry*.2016, 35, 277-28. DOI: <https://doi.org/10.1016/j.jiec.2016.01.005>.
- [26]Tasrina,R.C.; Acher,T.; Amin,M.N.; Quraishi,S.B.; Mustafa,A. I. Removal of Arsenic (III) from Groundwater by Adsorption onto Duckweed (Lemna minor). *International Research Journal of Pure et Applied Chemistry*.2015, 6, 120-127.<https://doi.org/10.9734/IRJPAC/2015/12798>.
- [27] Alhaji,M.I.N.; Tajun,M.B.M.K. Optimization and Kinetic Study for the Removal of Chromium (VI) Ions by Acid Treated Sawdust Chitosan Composite Beads. *International Research Journal of Pure and Applied Chemistry*.2014, 5, 160–176. <https://doi.org/10.9734/IRJPAC/2015/13834>.
- [28] Rahman,M.; Lamb,D.; Rahman,M.; Bahar,M.; Sanderson,P. Adsorption-Desorption Behavior of Arsenate Using Single and Binary Iron-Modified Biochars: Thermodynamics and Redox Transformation. *Journal of American Chemical Society Omega*.2022, 7, 101-117. <https://doi.org/10.1021/acsomega.1c04129>.
- [29] Langmuir,I. The adsorption of gases on plane surfaces of glass, mica and platinum. *Journal of American Chemical Society*.1918, 40, 1361–1403, <http://dx.doi.org/10.1021/ja02242a004>.
- [30] Melisa,A.; Indira,S.; Amra,O.; Edisa,P.;Husejin,K.; Abdel,D.; Halid,J.The Potential of Bentonite as a Low-cost Adsorbent for the Removal of Heavy Metal Ions from Multicomponent Aqueous Systems of the Galvanic Industry. *International Research Journal of Pure et Applied Chemistry*.2024, 25, 28-39.<https://doi.org/10.9734/IRJPAC/2024/v25i2848>.
- [31] Hema,K.R.Comparative Studies of Isotherm and Kinetics on the Adsorption of Cr (VI) and Ni (II) from Aqueous Solutions by Powder of Mosambi Fruit Peelings. *International Research Journal of Pure and Applied Chemistry*.2013, 4, 26–45. <https://doi.org/10.9734/IRJPAC/2014/5765>.